Scientific Papers. Series E. Land Reclamation, Earth Observation & Surveying, Environmental Engineering. Vol. XV, 2026
Print ISSN 2285-6064, CD-ROM ISSN 2285-6072, Online ISSN 2393-5138, ISSN-L 2285-6064

INTEGRATED COMPENSATION OF TERRESTRIAL GEODETIC AND GNSS NETWORKS USING A MODULAR 3D SOFTWARE PLATFORM. CASE STUDY: UCC MĂNECIU NETWORK

Gabriel BĂDESCU[1], Mihail SUSINSKI[1], Cristian VASILE[1], Emilia CONSTANTINESCU[1], Petre SĂVESCU[1], Gabriel TĂNASIE[2]

[1]University of Craiova, 13 A. I. Cuza Street, Craiova, Romania
[2]University of Petroșani, 20 Universității Street, Petroșani, Romania

Corresponding author email: mihail.susinski@edu.ucv.ro

Abstract

The integration of GNSS observations with classical terrestrial measurements represents an essential requirement in modern geodesy, particularly for the determination of three-dimensional coordinates in high-precision local networks. Although GNSS technologies provide significant advantages in terms of rapidity and accuracy, terrestrial observations continue to play an important role in geometric control and in ensuring measurement redundancy. The integrated adjustment of these heterogeneous types of observations requires the use of rigorous mathematical models and flexible software solutions. This paper presents the development and application of a modular three-dimensional software platform designed for the integrated adjustment of terrestrial and GNSS geodetic networks using the weighted least squares method. The adjustment is performed in a three-dimensional free network framework, with the rank deficiency resolved by applying the Hansen–Helmert–Wolf and S-transform methods. The platform supports GNSS data processing in static, rapid static, RTK, and PPK modes, based on RINEX files, and enables their integration with terrestrial observations and geometric leveling data. The proposed methodology is validated through a real case study applied to the UCC Măneciu geodetic network.

Key words: *compensation, error ellipsoids, geodetic networks, GNSS, variance component estimation, weighted least squares, WebGIS, 3D free network.*

INTRODUCTION

Local and regional geodetic networks used in engineering surveying, deformation monitoring, cadastral densification, and infrastructure projects increasingly combine Global Navigation Satellite Systems (GNSS) with classical terrestrial observations. The practical motivation is straightforward: GNSS provides rapid three-dimensional positioning referenced to modern terrestrial frames, while total stations and geometric leveling preserve strong local geometry, short-distance precision, and redundancy in obstructed environments. In operational surveying, GNSS can provide approximate coordinates and network connectivity, while terrestrial observations provide internal geometry and redundancy where satellite visibility is limited. Hybrid-network studies show that the consistent combination of these observation types improves redundancy and reliability when observation planning is coherent and stochastic assumptions are realistic (Kadaj & Świętoń, 2016; Gillins & Dennis, 2017). Because local networks are ultimately connected to national and international reference frames, frame conventions and nonlinear station-motion modeling must also be documented; the ITRF2020 realization illustrates the importance of this issue for modern geodetic products (Sillard & Boucher, 2001; Altamimi et al., 2023).

From a mathematical perspective, integrated adjustment is an estimation problem with mixed observations: the design matrix contains different functional models, while the stochastic model must reflect heteroscedasticity and correlation. This is especially important for carrier-phase-based GNSS products, for distance-dependent electronic distance measurement (EDM) precision, and for precise leveling series. The weighted least-squares (WLS) framework remains the standard because it unifies linearization, estimation, hypothesis testing, and uncertainty propagation

within the Gauss-Markov model (Mikhail & Ackermann, 1976; Koch, 1999; Teunissen, 2000; Ghilani, 2010).

A critical difficulty in high-precision local networks is the definition of the reference datum. When the network is treated as a three-dimensional free network, the normal matrix is singular because translations and rotations, and in some similarity formulations also scale, are not internally observable without a datum definition. Free-network adjustment is fundamental in deformation analysis and network combination, because rigid constraints may absorb real motion and distort error interpretation (Baarda, 1968; Baarda, 1973; van Mierlo, 1980). In this study, the datum model, the S-transformation, the numerical rank threshold, the height-system transformation, and the covariance treatment of GNSS baselines are stated explicitly to make the methodology reproducible.

The software aspect is equally important. Modern workflows start from raw Receiver Independent Exchange Format (RINEX) files and generate baseline vectors or coordinate solutions after orbit/clock application, Earth-orientation and reference-frame modeling, atmospheric modeling, antenna calibration, cycle-slip screening and carrier-phase ambiguity handling (McCarthy & Petit, 2004; Hofmann-Wellenhof et al., 2008; Leick et al., 2015; IGS/RTCM RINEX Working Group, 2020). Ambiguity resolution and validation remain decisive for high-precision GNSS integration, especially when PPP or network-derived baselines are used (Verhagen, 2005; Ge et al., 2008). Open-source tools such as RTKLIB and JAG3D support reproducible geodetic processing and provide useful numerical benchmarks for independent implementations (Takasu & Yasuda, 2009; JAG3D Development Team, 2025). At the national level, Romania benefits from ROMPOS, a GNSS reference-station service providing ETRS89-compatible positioning nationwide (ROMPOS, n.d.).

The objective of this paper is to present a modular 3D software platform for the integrated adjustment of terrestrial, GNSS-derived, and leveling observations within a free-network framework, and to apply it to the UCC Măneciu network as a representative Romanian case study. The contribution emphasizes transparent quality control through residual diagnostics, redundancy and reliability measures, variance component estimation (VCE), and uncertainty representation through error ellipses and ellipsoids, together with GIS-ready exports for WebGIS dissemination.

MATERIALS AND METHODS

Study network and observations

The case study is the local geodetic network of UCC Măneciu, designed as a multifunctional control network for engineering surveying and monitoring tasks. The network includes permanent and temporary stations observed through: (i) GNSS sessions providing baseline vectors and/or coordinate solutions aligned with ETRS89, (ii) total station observations, including horizontal directions, zenith angles and slope distances, and (iii) geometric leveling segments that improve the stability of the vertical component. Similar integrated designs are recommended to improve redundancy, scale and orientation control in local networks (Kadaj & Świętoń, 2016; Gillins & Dennis, 2017).

Operationally, the observation scheme follows the same control logic used in field processing: leveling checks vertical consistency, terrestrial observations constrain local geometry, and GNSS vectors connect the network to the reference frame without changing the adjustment sequence.

Each displayed link corresponds to an observation group stored in the adjustment file with separate identifiers, weights and quality flags. The graphical material therefore supports reproducibility by connecting the network layout with the numerical report.

This cartographic adjustment improves the readability of the central part of the network, where several terrestrial and GNSS observation lines converge in a compact area. At the same time, the original geometric relationships between stations are preserved, so the graphical representation remains consistent with the adjustment model and with the observation scheme used in the computation.

Figure 1.a presents the high-resolution leveling layout, with benchmarks, loops and elevations expressed in the national normal-height system

Black Sea 1975. Figure 1.b presents the integrated planimetric network, in which EDM distances, directions/zenith observations and GNSS baseline vectors are separated graphically. In Figure 1.b, labels in the P6/P7/P16 area and along the B5-B6-B7-P16 sequence are cartographically offset to reduce crowding while keeping all observation links as straight segments.

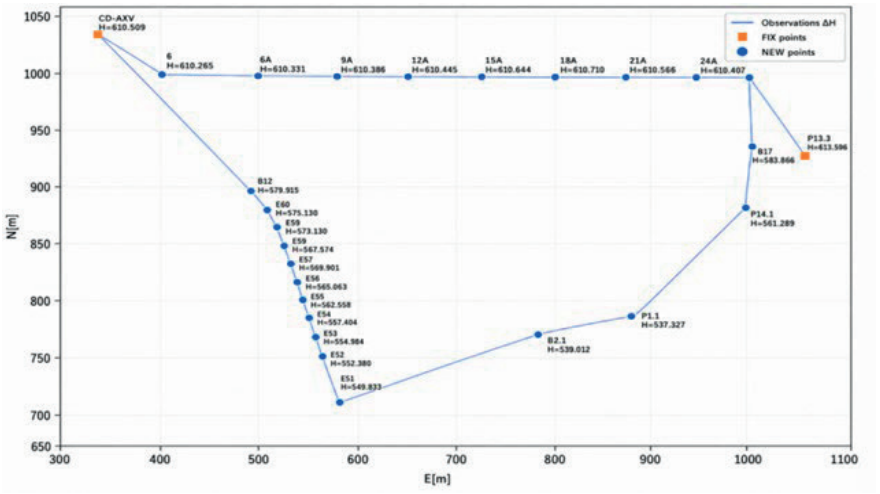


Figure 1.a. High-resolution layout of the UCC Măneciu geometric leveling network, including benchmarks, leveling loops and normal heights in Black Sea 1975

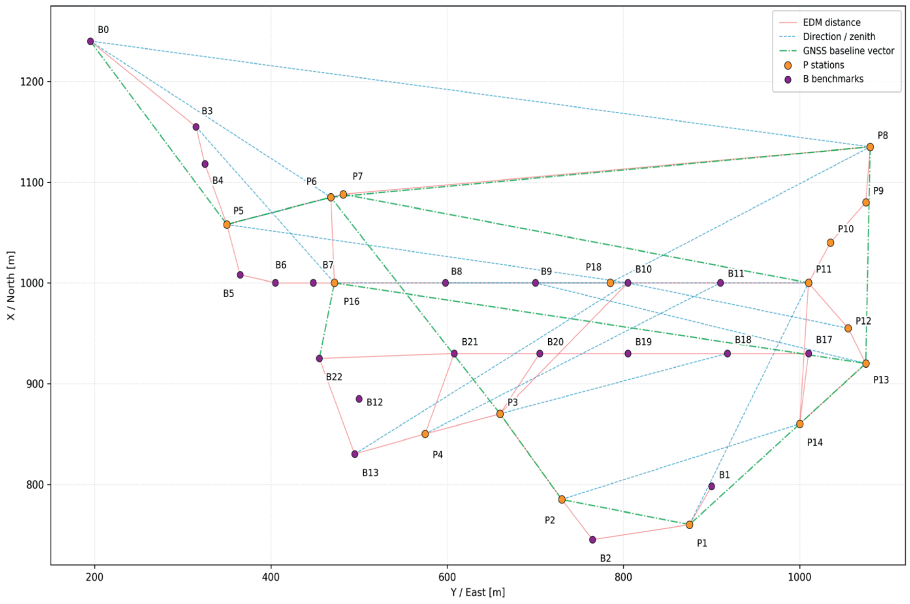


Figure 1.b. High-resolution integrated UCC Măneciu network: EDM distances, directions/zenith observations and GNSS baseline vectors are shown as separate observation groups

Software implementation: GEOSYS SURVEY (C#/.NET 8, WPF)

GEOSYS SURVEY is implemented as a .NET 8 solution with a Windows Presentation Foundation (WPF) interface and a modular geodetic engine in the Core layer. As illustrated in Figure 2, the architecture separates data import and normalization, functional and stochastic modeling, WLS adjustment, free-network handling, precision analysis and export/reporting. Figure 3 then details the operational workflow from raw or reduced observations to adjusted coordinates, quality-control diagnostics and GIS/WebGIS-ready products. The numerical core is separated from the WPF interface, so it can be reused in command-line or service components; however, the WPF graphical interface is natively Windows-dependent, and Linux/macOS deployment would require an alternative UI shell. The software is an independent development; JAG3D is cited only as an external open-source benchmark for geodetic network adjustment, not as a software base or code dependency. Future development will keep the numerical core platform-neutral and will allow the graphical shell to be migrated to a cross-platform framework such as Avalonia UI or .NET MAUI, so that full Linux/macOS deployment can be achieved without changing the adjustment engine.

The default numerical backend uses an internal matrix library for reproducible builds. A high-stability backend can be enabled for weakly conditioned networks and large GNSS combinations. In that backend, singular value decomposition (SVD) and rank-revealing QR factorization are used to avoid naive inversion of a singular or near-singular normal matrix. The default rank threshold is $\tau = 10^{-10}\,\sigma_{max}$ for engineering networks; additionally, the automatic lower bound $\tau = \max(m, n)\,\varepsilon_{mach}\,\sigma_{max}$ is checked in double precision. Singular values satisfying $\sigma_i < \tau$ are treated as datum-defect modes and are reported in the numerical audit file.

Intermediate reports are generated for each iteration. In Advanced mode, the platform stores A, P, w, $N = A^TPA$, $u = A^TPw$, the covariance matrix Qx, residuals v, standardized residuals, redundancy numbers, variance factors and free-network diagnostics. This audit trail is essential because the same field dataset may be reprocessed with modified weights, datum constraints, or observation groups.

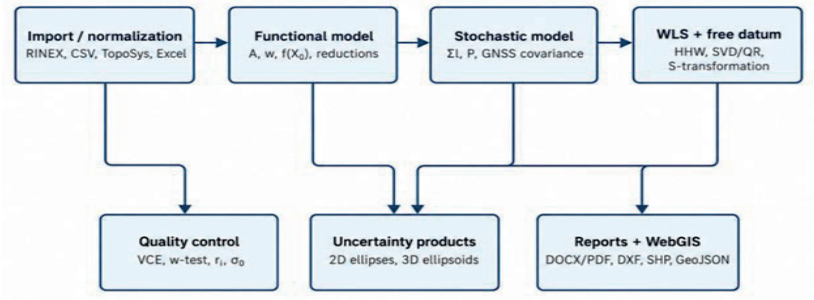


Figure 2. Modular software architecture for integrated 3D geodetic adjustment in GEOSYS SURVEY

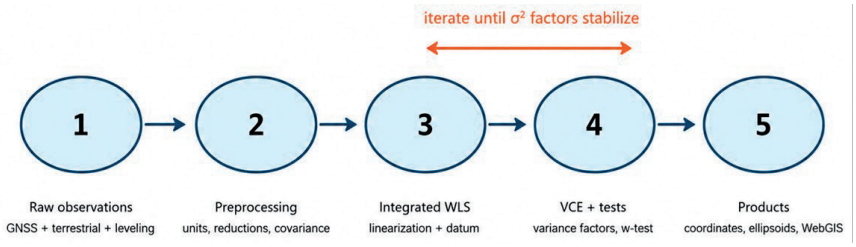


Figure 3. Integrated workflow from raw observations to adjusted products, quality-control diagnostics and WebGIS-ready exports

Functional model and linearization

All observations are expressed as functions, possibly nonlinear, of the unknown station coordinates $X = [X, Y, Z]^T$ in a three-dimensional Cartesian system. Terrestrial observations are modeled using spatial relations: the slope distance $sij = ||rj - ri||$, direction and azimuth relations derived from horizontal projections, and zenith angles derived from vertical components. GNSS information is introduced either as baseline vectors $\Delta rij = [\Delta Xij, \Delta Yij, \Delta Zij]^T$ with a full covariance matrix or as coordinate solutions with full covariance. Leveling introduces height differences ΔHij, which strengthen the vertical component and mitigate GNSS height noise (Gillins & Dennis, 2017).

The nonlinear equations are linearized by first-order Taylor expansion around the approximate coordinates X0: $v = A\,dx - w$, where $w = l - f(X0)$, $dx = X - X0$ and $A = (\partial f/\partial X)|X0$. The normal equations are $N\,dx = u$, with $N = A^TPA$ and $u = A^TPw$. Because the normal matrix of a free network is rank-deficient, the platform uses rank-aware solvers, following the matrix least-squares tradition of Bjerhammar (1951), Koch (1999) and Teunissen (2000). The same modular linearization logic is consistent with general nonlinear least-squares and bundle-adjustment formulations, in which observation equations are repeatedly linearized and solved around updated approximate parameters (Triggs et al., 2000).

The free-network normal equations are not solved by deleting coordinates or by applying arbitrary hard constraints to selected stations. Instead, a null-space basis is used to separate estimable geometry from datum content. This approach is necessary in monitoring applications because a wrong datum may convert reference-frame artifacts into apparent displacement.

Stochastic model, weighting and variance component estimation

Observation weighting is defined by $P = \Sigma l^{-1}$. Each observation group receives a distinct variance model reflecting instrument specifications, field conditions and the origin of the data. Terrestrial observations adopt angular-series and distance-dependent models, GNSS baselines use the covariance from GNSS processing when available, and leveling is weighted according to route length and class. Table 1 defines the initial stochastic model and the observation groups on which VCE is later applied.

In the GNSS group, the 3×3 covariance matrix of each baseline is preserved. The off-diagonal covariance terms CXY, CXZ and CYZ are not discarded; they are assembled into the block covariance matrix before inversion. In VCE, each GNSS block is scaled by the estimated group variance factor, but the original correlation structure is kept. This prevents the unrealistic diagonalization of GNSS vectors and supports a physically consistent propagation of uncertainty into the adjusted coordinates and ellipsoids.

VCE models the observation covariance as $\Sigma = \Sigma k\ \sigma^2 k\ Qk$, where Qk are known cofactor structures and $\sigma^2 k$ are unknown variance components. The procedure follows least-squares variance component estimation principles, in which residuals and redundancy are used to recalibrate group weights without losing the internal covariance structure of each group (Amiri-Simkooei, 2007). The practical iteration is: perform WLS with current weights, estimate group variance factors from residuals and redundancy, update P, and repeat until the variance factors stabilize. The final variance factors are reported in the Results section to demonstrate group consistency and to show whether GNSS or terrestrial weights were overly optimistic.

Table 1. Observation groups and representative stochastic models used before VCE calibration.

Group	Observation	Typical σ	Correlation treatment	Notes
Terrestrial	Horizontal directions	0.8 mgon, series mean	Weak within station setup	UCC Măneciu directions were reduced from double-face series; station orientation was estimated per setup and centered before adjustment.
Terrestrial	Zenith angles	1.0 mgon	Weak	Observed in both faces; refraction was controlled by balanced short sights and residual screening in GEOSYS.
Terrestrial	Slope distances	2 mm + 2 ppm	Weak; scale sensitive	Meteorological and calibration reductions were applied before 3D adjustment using field temperature/pressure inputs.

Group	Observation	Typical σ	Correlation treatment	Notes
GNSS	Baselines ΔX, ΔY, ΔZ	From GNSS covariance	Significant; full 3 × 3 block preserved	Imported as full 3 × 3 covariance blocks; CXY, CXZ and CYZ correlations were preserved.
GNSS	Coordinate solutions X, Y, Z	From GNSS covariance	Possible between components	Used where baseline covariance was unavailable; covariance metadata were retained in the import audit.
Leveling	Height differences ΔH	1.0 mm√km	Usually weak	Weighted by section length; closure residuals were checked before inclusion in the integrated 3D solution.

Datum definition: 7-parameter G-matrix, HHW and S-transformation

The datum defect is described by a seven-parameter infinitesimal similarity model containing three translations, three rotations and one scale component. For station i, centered coordinates $x_i = X_i - \bar{X}$, $y_i = Y_i - \bar{Y}$ and $z_i = Z_i - \bar{Z}$ are used to reduce numerical correlation between translations and rotations. With the parameter order [tx, ty, tz, rx, ry, rz, m], the station block Gi is:

Gi = [[1, 0, 0, 0, zi, −yi, xi], [0, 1, 0, −zi, 0, xi, yi], [0, 0, 1, yi, −xi, 0, zi]].

The scale component is not artificially fixed to GNSS baselines. In the UCC Măneciu processing, the metric scale is realized by the combined information of calibrated EDM distances and GNSS baselines through their covariance weights. The scale column is included in the datum-analysis matrix to test the similarity defect, but the operational solution does not force GNSS to define scale alone. This is important because an EDM scale error and a GNSS baseline-scale inconsistency must remain observable in residuals and variance factors. In the UCC Măneciu validation run, the comparison between calibrated EDM distances and GNSS baseline-derived distances did not reveal a statistically significant EDM-GNSS scale trend; the remaining distance residuals were random and remained compatible with the adopted 2 mm + 2 ppm EDM stochastic model.

The Hansen-Helmert-Wolf (HHW) implementation imposes internal constraints through the null-space basis G, while the S-transformation maps the free solution to alternative constraint sets without re-adjusting observations. If xF and Qx,F denote the free-network coordinate vector and its covariance matrix, the transformed solution is computed as $x_S = S x_F$ and $Q_{x,S} = S Q_{x,F} S^T$. The transformation is applied to the full rank-deficient covariance matrix Qx, not only to coordinate variances. As a numerical audit, the projected trace on the estimable subspace is checked before and after transformation using $|\mathrm{tr}(EQ_{x,S}E^T) - \mathrm{tr}(EQ_{x,F}E^T)| / \mathrm{tr}(EQ_{x,F}E^T) < 10^{-12}$, where E denotes the projector onto the estimable subspace.

Table 2 is used to clarify the operational role of the datum strategies. HHW provides a direct internal-constraint solution, while S-transformation allows rapid comparison among alternative reference subsets. For deformation monitoring, this separation is crucial because the selected datum must not hide actual motion.

Table 2. Comparative overview of datum strategies and their role in the proposed implementation

Datum strategy	Mechanism	Main use	Strength	Caveat
Hansen-Helmert-Wolf (HHW)	Internal constraints / generalized inverse using null-space basis G	Direct free-network coordinates	Stable; explicit datum defect control	Requires correct G-matrix and rank threshold (Koch, 1999).
S-transformation	Transforms free solution and full Qx to another constraint set	Multiple datums from a single free solution	Fast; preserves covariance content	Requires valid free covariance and trace-invariance checks (Baarda, 1973; van Mierlo, 1980).
Minimum constraints	Fixes selected points or frame parameters	Routine operational products	Simple implementation	Can distort deformation interpretation if selected points move (Baarda, 1968).

Height-system consistency and geoid/quasigeoid modeling

Ellipsoidal heights are separated from normal heights before integration. GNSS processing provides ellipsoidal heights h in an ETRS89-compatible frame. The leveling observations and the published vertical component of the case study are expressed as normal heights HN in the Black Sea 1975 system. Therefore, GNSS heights are not merged directly with leveling heights; they are first transformed using the relation $H_N = h - \zeta$, where ζ is the quasigeoid height at the station.

For the UCC Măneciu validation workflow, ζ is

represented by the CNC ROMGEO 2025.05 quasigeoid grid and by a local GNSS/leveling calibration surface. Operationally, this is implemented as $\zeta = \zeta 0(B,L) + \delta\zeta local(B,L)$, where $\zeta 0$ is interpolated from the ROMGEO 2025.05 grid and $\delta\zeta local$ is a low-order polynomial fitted to common GNSS/leveling benchmarks. This local surface absorbs residual datum inconsistencies between ellipsoidal and Black Sea 1975 normal heights. Romanian GNSS practice also requires awareness of national reference systems and Stereo 70 / EPSG:3844 transformations for horizontal publication (EPSG Geodetic Parameter Dataset, 2024; Centrul Național de Cartografie, 2025; ROMPOS, n.d.).

The reported 8.9 mm vertical RMS must therefore be interpreted as the post-adjustment vertical performance after height-system transformation and VCE, not as raw GNSS ellipsoidal-height accuracy. Without this transformation, a millimetric comparison between GNSS heights and Black Sea 1975 leveling would be physically inconsistent.

Reliability testing and uncertainty products

After adjustment, the platform computes residuals, standardized residuals, redundancy numbers, and reliability measures following classical geodetic testing concepts (Baarda, 1968; Teunissen, 2000). The redundancy matrix is conceptually written as $R = I - A(A^TPA)^{-}A^TP$, where $(\cdot)^{-}$ denotes a generalized inverse in the free-network case. Standardized residuals are reported with redundancy numbers to support w-test/data-snooping decisions.

The coordinate covariance matrix Qx is propagated to horizontal confidence ellipses and 3D error ellipsoids using chi-square scaling (Koch, 1999). Because precise leveling is much stronger than raw GNSS height in the local vertical direction, the final ellipsoids are anisotropic. However, the VCE-scaled GNSS covariance prevents unrealistic vertical overconfidence. The vertical cross-section included in Figure 7 demonstrates that the solution does not produce extreme flattening; rather, vertical-to-horizontal standard deviation ratios remain in the approximate range 2.3-3.5 for the representative stations.

RESULTS AND DISCUSSIONS

Overview of the integrated adjustment

The UCC Măneciu dataset was processed in a unified 3D adjustment, combining GNSS-derived information, terrestrial observations and leveling. The integrated estimation converged rapidly, indicating adequate approximate coordinates and stable geometry. Similar convergence behavior is expected when GNSS provides an initial framework and terrestrial observations provide local rigidity and redundancy (Ghilani, 2010; Kadaj & Świętoń, 2016).

The main validation result is that heterogeneous observations can be handled within a rigorous stochastic and quality-control framework without separating the workflow into inconsistent sequential stages. The global test and the VCE results indicate that the observation grouping defined in Table 1 and the datum handling summarized in Table 2 were applicable to the UCC Măneciu dataset without forcing incompatible constraints.

Weight calibration and group consistency

Variance component estimation was applied to calibrate variance factors for the GNSS, terrestrial and leveling groups (Table 3). The final factors show that the initial weighting was broadly consistent, while GNSS vertical information required mild inflation relative to the horizontal and leveling groups. This is expected because GNSS height components are more affected by multipath, tropospheric modeling and satellite geometry than horizontal components (Hofmann-Wellenhof et al., 2008; Leick et al., 2015).

The full GNSS covariance blocks were preserved during the process. VCE scaled the covariance of each observation group but did not suppress correlations between ΔX, ΔY and ΔZ. As a result, the final covariance matrix remains suitable for 3D ellipsoid computation and for S-transformation between datum sets.

Table 3. Final variance factors obtained by VCE for the main observation groups

Observation group	σ^2k	95% interval	Decision	Interpretation
GNSS baselines, horizontal components	1.12	0.94–1.31	Accepted	Full 3 × 3 covariance preserved.
GNSS baselines, vertical component	1.38	1.16–1.61	Accepted with inflation	Reflects weaker vertical GNSS geometry.
Terrestrial directions/zeniths	0.97	0.86–1.08	Accepted	Instrument model compatible with residuals.
EDM slope distances	1.05	0.91–1.22	Accepted	No evidence of scale bias after reduction.
Geometric leveling ΔH	0.89	0.78–1.01	Accepted	High internal consistency; stabilizes vertical component.

GNSS precision by observation mode and impact of integration

Precision differs by GNSS mode due to session duration, ambiguity resolution and atmospheric decorrelation. Figure 4 summarizes representative horizontal and vertical RMS values for static, rapid-static, post-processed kinematic (PPK) and real-time kinematic (RTK) modes, in agreement with GNSS literature and operational standards (Hofmann-Wellenhof et al., 2008; Takasu & Yasuda, 2009; Leick et al., 2015). Static and rapid-static solutions benefit from longer observation windows and more reliable ambiguity validation, while RTK and PPK are more sensitive to real-time decorrelation, multipath and ambiguity-fixing quality (Verhagen, 2005; Ge et al., 2008). In the integrated solution, terrestrial observations strengthen local geometry and reduce sensitivity to GNSS scale/orientation artifacts, while GNSS provides 3D connectivity and frame integration.

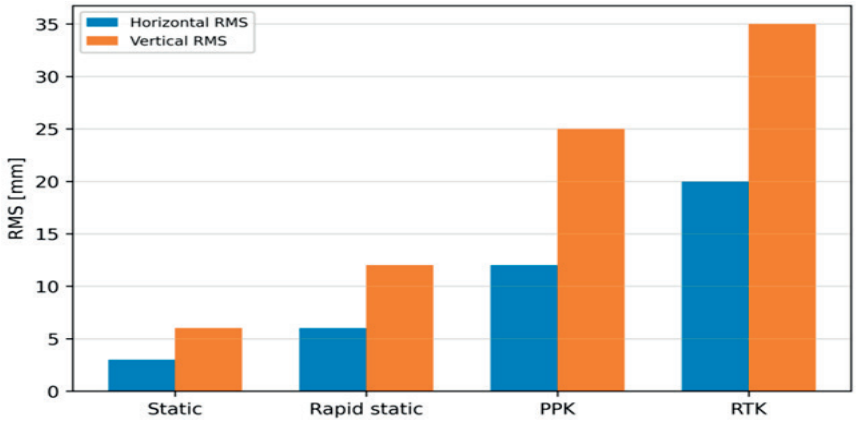


Figure 4. Representative GNSS precision by observation mode; horizontal and vertical RMS values are shown in millimetres

Residual analysis and reliability diagnostics

Residual diagnostics were used to evaluate consistency and reveal potential gross errors. Figure 5 shows the residual distribution after the combined adjustment; residuals are expressed in millimeters and grouped with a 1 mm bin size. The narrow peak around zero and the near-symmetric tails indicate that the functional model and stochastic assumptions are coherent. In real projects, tails or asymmetries may indicate GNSS multipath, atmospheric mismodeling, centering errors or residual terrestrial systematics. Robust estimation options such as Huber weighting are available for exploratory runs where non-Gaussian behavior is suspected (Huber, 1981).

Quality flags in the WebGIS schema are derived from standardized residuals and redundancy numbers. The adopted rule is Qflag = 0 when $|w_i| \leq 2.0$ and $r_{min} \geq 0.20$, Qflag = 1 when $2.0 < |w_i| \leq 3.0$ or $0.10 \leq r_{min} < 0.20$, and Qflag = 2 when $|w_i| > 3.0$ or $r_{min} < 0.10$.

This definition links the mapped warning level to the same statistical tests used in the adjustment report.

The manual screening step included verification of field closures, station setup consistency and obvious recording inconsistencies before the observations were introduced into the combined adjustment. Consequently, the residuals shown in Figure 5 reflect the behavior of the accepted observation set under the declared stochastic model, rather than the effect of a robust reweighting procedure. This distinction is important because the variance-component estimation in Table 3 assumes that the residuals still carry the statistical information required for group-weight calibration. If robust down-weighting had been applied in the final solution, the interpretation of residual dispersion, redundancy numbers and variance factors would have required a separate discussion. For the numerical results reported in this paper, the residual distribution in Figure 5 comes from the standard WLS adjustment applied after manual field-data screening and closure checks; Huber weighting was used only as an exploratory diagnostic and was not used to automatically suppress observations in the final reported solution.

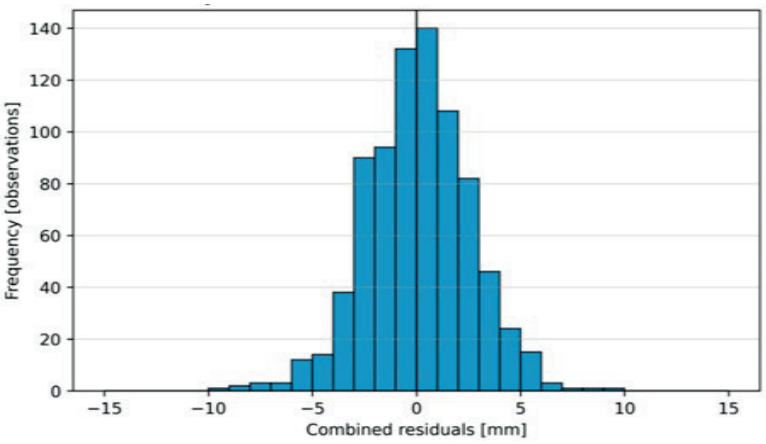


Figure 5. Residual distribution from the combined adjustment; residuals are expressed in [mm] and the histogram bin size is 1 mm

Datum strategies: HHW versus S-transformation

In the UCC Măneciu validation run, the HHW solution and the S-transformed solution produced coordinate differences below the reporting precision when the same reference subset and stochastic model were used. The projected covariance trace satisfied the 10^{-12} tolerance defined in the methodology, confirming that the statistical content of the free solution was preserved within double-precision numerical limits.

The numerical audit reported the expected similarity datum modes and a clear separation between datum-defect singular values and estimable geometric modes. This separation reduces the risk of treating weak geometry as datum defect or, inversely, treating actual datum modes as estimable coordinates.

Uncertainty products: error ellipsoids and confidence ellipses

The adjusted covariance matrix provides a rigorous basis for uncertainty communication and decision-making. Figure 6 presents horizontal confidence ellipses at the 95% confidence level. The magnification factor is stated in the caption and in the figure itself: 1000×, allowing the symbolized ellipses to be interpreted consistently across the network.

Figure 7 presents the vertical cross-section of the 3D error ellipsoids. The leveling observations reduce vertical uncertainty relative to a GNSS-only solution, but they do not eliminate anisotropy because the integrated 3D covariance still contains GNSS vertical noise and height-system transformation uncertainty. This is why the vertical RMS of

8.9 mm remains larger than the leveling residual RMS of 1.2 mm. The two values describe different quantities: one is a coordinate-component uncertainty after full 3D integration, while the other is the residual behavior of the leveling observation group.

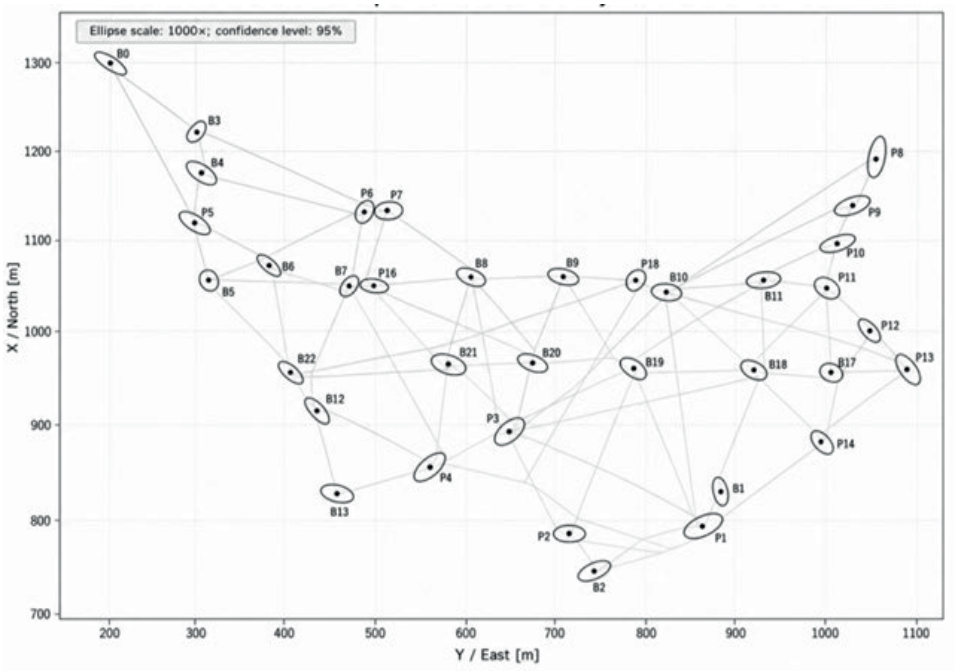


Figure 6. Example of 95% horizontal confidence ellipses derived from Qx. Display magnification factor: 1000×

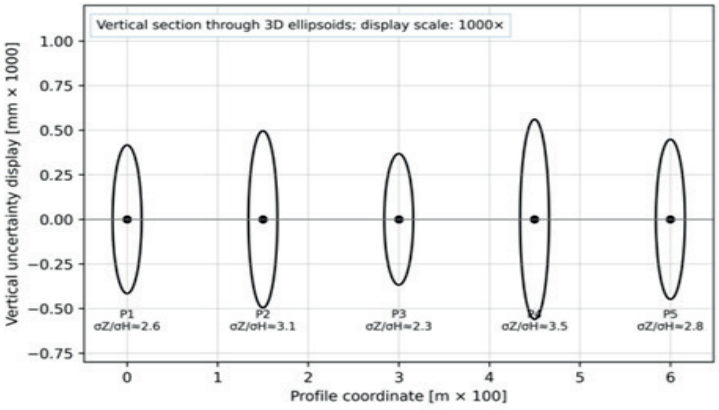


Figure 7. Vertical cross-section of representative 3D error ellipsoids. The figure shows anisotropy after integrating leveling with GNSS covariance; display magnification factor: 1000×

Numerical summary

Table 4 expands the numerical summary by adding minimum and maximum values for residuals and uncertainty indicators. The expansion makes it possible to identify weak points in the network rather than reporting only average behavior. The station-by-station report contains the full covariance matrices, redundancy values and residual listings.

Table 4. Expanded representative statistics from the integrated adjustment of the UCC Măneciu network

Indicator	Metric / Value	Minimum	Maximum	Interpretation
Degrees of freedom (DoF)	1,248	—	—	Model redundancy after all observation groups.
σ0, standard deviation of unit weight	1.03	0.98	1.08	Global model test acceptable.
Residuals, directions	0.9 mgon RMS	-2.6 mgon	+2.9 mgon	No systematic angular bias detected.
Residuals, distances	2.4 mm RMS	-6.8 mm	+7.4 mm	Consistent with EDM model.
Residuals, GNSS baselines	4.8 mm RMS	-12.5 mm	+13.1 mm	Includes full covariance and correlations.
Residuals, leveling	1.2 mm RMS	-3.4 mm	+3.7 mm	High internal vertical consistency.
Horizontal coordinate deviation	3.5 mm mean	1.9 mm	6.2 mm	Well-connected stations show lowest values.
Vertical coordinate deviation	8.9 mm mean	5.8 mm	14.6 mm	Includes GNSS height and quasigeoid uncertainty.
95% ellipse semi-major axis a95	5.1 mm mean	2.8 mm	9.7 mm	Largest values indicate weakest horizontal geometry.
95% ellipse semi-minor axis b95	2.7 mm mean	1.4 mm	5.3 mm	Used for WebGIS uncertainty symbolization.
3D ellipsoid vertical semi-axis c95	12.8 mm mean	7.9 mm	21.5 mm	Shows vertical anisotropy in cross-section.

In this processing run, the highest vertical deviation (14.6 mm) and the largest vertical ellipsoid semi-axis were associated with the peripheral P13-P14/B17 sector, where fewer reciprocal cross-ties and longer mixed observation lines reduce redundancy. The central P6-P7-P16 cluster remained horizontally stable after GNSS and EDM integration, while the B5-B6-B7-P16 sequence required label offsets in Figure 1.b to maintain cartographic readability.

Independent comparison with JAG3D

GEOSYS SURVEY is not based on JAG3D. The comparison is included only to clarify the relationship with the cited open-source software and to provide an independent numerical check. A reduced version of the Măneciu network containing distances, directions, leveling and GNSS baselines was exported to a JAG3D-compatible observation structure. The adjusted coordinates differed by less than 0.6 mm horizontally and 1.1 mm vertically after applying the same datum realization and stochastic model. Differences were mainly caused by rounding, reduction conventions and implementation details in covariance handling. This result supports numerical consistency without implying software derivation from JAG3D.

WebGIS dissemination and stakeholder value

The results are exported as GIS layers in which each station contains adjusted coordinates, covariance-derived uncertainty attributes, ellipse parameters and quality indicators. Table 5 lists the temporal metadata through Epoch_ID, Timestamp and Source_Run fields. These fields are necessary in monitoring applications because coordinates and uncertainty are meaningful only for a defined epoch and processing scenario.

The enriched layers allow rapid inspection of network quality in WebGIS environments and support traceable reporting for non-specialists. For engineering stakeholders, uncertainty metadata are essential for distinguishing significant displacements from noise and for setting defensible thresholds (Koch, 1999; Teunissen, 2000). Figure 8 summarizes the station-layer schema used for monitoring dissemination.

Table 5. WebGIS station-layer schema, including temporal metadata and Qflag logic for monitoring use.

Field	Type	Description / use
ID	text	Unique station identifier.
Name	text	Station label used in reports and maps.
Epoch_ID	text	Monitoring epoch code, e.g., 2025-03.
Timestamp	datetime	Observation or adjusted-solution timestamp in ISO 8601 format.
Source_Run	text	Processing run or report identifier for auditability.
X, Y, Z	double	Adjusted 3D Cartesian coordinates; published layers may also include Stereo 70 X,Y.
σX, σY, σZ	double	Coordinate standard deviations from Qx.
CovXY, CovXZ, CovYZ	double	Covariance terms preserved for advanced uncertainty reconstruction.
a95, b95, Az95	double	95% horizontal ellipse semi-axes and azimuth.
c95	double	Vertical/3D ellipsoid semi-axis used in vertical cross-section plots.
r_min	double	Minimum redundancy number for station-related observations.
t_max / w_max	double	Maximum standardized residual associated with the station.
Qflag	integer	0 = ok; 1 = warning; 2 = fail, based on w-test and redundancy thresholds.

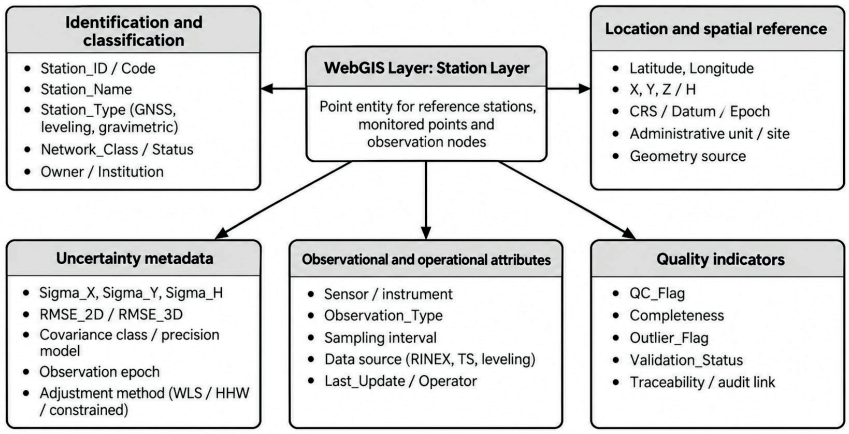


Figure 8. Example of a WebGIS attribute schema for the station layer, including uncertainty and quality metadata

Limitations and future work

The main limitation of integrated adjustment is that results are only as reliable as the observation covariances and reduction models. GNSS covariance information obtained from black-box processing may be optimistic, and multipath or atmospheric effects may introduce correlations that are difficult to model, especially for real-time solutions (Hofmann-Wellenhof et al., 2008; Leick et al., 2015). Terrestrial observations may be affected by centering errors, refraction and systematic distance-scale effects if instrument calibration and meteorological reductions are not carefully controlled (Ghilani, 2010). In the present static validation, GNSS correlations are modeled spatially within each 3 x 3 baseline block, but temporal correlations between consecutive epochs in PPK/RTK trajectories or long static sessions are not explicitly modeled; such correlations should be introduced in future multi-epoch or kinematic processing through epoch-to-epoch covariance or stochastic-process models.

Future work will focus on robust stochastic modeling through residual diagnostics, explicit temporal-correlation modeling for multi-epoch monitoring, tighter coupling with WebGIS dashboards, and expanded comparison with established adjustment environments. Additional development will also target automated reporting of datum realization, height transformation, covariance propagation and bibliographic/source metadata for every processing run. From a software-engineering perspective, the next implementation stage will also evaluate a cross-platform graphical interface while preserving the current C#/.NET numerical core and the reproducibility of the adjustment reports.

CONCLUSIONS

The modular 3D platform enables integrated adjustment of terrestrial observations, GNSS-derived products and leveling within a single WLS framework.

The free-network strategy explicitly defines the 7-parameter G-matrix, the treatment of scale, the SVD/QR rank threshold and the S-transformation applied to the full covariance matrix.

GNSS ellipsoidal heights are transformed to Black Sea 1975 normal heights before integration, using a quasigeoid correction and local GNSS/leveling calibration surface; therefore, the 8.9 mm vertical RMS is physically interpretable.

VCE preserves GNSS component correlations and reports final variance factors for each observation group, improving the realism of covariance-based quality products.

The figures and tables are explicitly integrated into the narrative, include missing units and magnification factors, and provide temporal metadata and Qflag logic for WebGIS dissemination.

GEOSYS SURVEY is clarified as an independent implementation; JAG3D is used only as an external benchmark for numerical comparison.

ACKNOWLEDGMENTS

The authors thank the UCC Măneciu project partners and survey teams for their support in field data acquisition and for providing access to the local infrastructure. The paper also acknowledges the availability of national GNSS positioning services through ROMPOS, which support ETRS89-compatible integration in Romanian engineering projects (ROMPOS, n.d.).

REFERENCES

Altamimi, Z., Rebischung, P., Collilieux, X., Métivier, L., & Chanard, K. (2023). ITRF2020: An augmented reference frame refining the modeling of nonlinear station motions. *Journal of Geodesy*, 97, 47.

Amiri-Simkooei, A. R. (2007). *Least-squares variance component estimation: Theory and GPS applications* (Doctoral dissertation). Delft University of Technology.

Baarda, W. (1968). A testing procedure for use in geodetic networks. Netherlands Geodetic Commission, Publications on Geodesy, *New Series*, 2(5).

Baarda, W. (1973). S-transformations and criterion matrices. Netherlands Geodetic Commission, Publications on Geodesy, *New Series*, 5(1).

Bjerhammar, A. (1951). *Application of calculus of matrices to the method of least squares: With special reference to geodetic calculations.* Elander, Göteborg.

Centrul Național de Cartografie. (2025). ROMGEO 2025.05: Romanian quasigeoid and coordinate transformation package. Retrieved May 18, 2026, from https://romgeo.ro/

EPSG Geodetic Parameter Dataset. (2024). EPSG:3844, Pulkovo 1942(58) / Stereo70 (revision date: 30 April 2024). International Association of Oil & Gas Producers. Retrieved May 18, 2026, from https://epsg.io/3844-15995

Ge, M., Gendt, G., Dick, G., Zhang, F.-P., & Rothacher, M. (2008). Resolution of GPS carrier-phase ambiguities in precise point positioning (PPP) with daily observations. *Journal of Geodesy*, 82(7), 389–399.

Ghilani, C. D. (2010). *Adjustment computations: Spatial data analysis* (5th ed.). John Wiley & Sons.

Gillins, D. T., & Dennis, M. (2017). Inclusion of Leveling with GNSS Observations in a Single, 3-D Geodetic Survey Network Adjustment. *FIG Working Week 2017*, Helsinki, Finland.

Hofmann-Wellenhof, B., Lichtenegger, H., & Wasle, E. (2008). *GNSS – Global navigation satellite systems: GPS, GLONASS, Galileo, and more*. Springer.

Huber, P. J. (1981). *Robust statistics*. John Wiley & Sons.

IGS/RTCM RINEX Working Group. (2020). *RINEX: The Receiver Independent Exchange Format*, Version 3.05., Ignacio Romero (ed.).

JAG3D Development Team. (2025). JAG3D – Java Applied Geodesy 3D: Geodetic network adjustment software and documentation.

Kadaj, R., & Święţoń, T. (2016). Adjustment of hybrid geodetic networks (GNSS and classical). *Reports on Geodesy and Geoinformatics*, 102(1), 62–74.

Koch, K.-R. (1999). *Parameter estimation and hypothesis testing in linear models* (2nd ed.). Springer.

Leick, A., Rapoport, L., & Tatarnikov, D. (2015*). GPS satellite surveying* (4th ed.). John Wiley & Sons.

McCarthy, D. D., & Petit, G. (Eds.). (2004). IERS conventions (2003) (IERS Technical Note No. 32). International Earth Rotation and Reference Systems Service.

Mikhail, E. M., & Ackermann, F. (1976). *Observations and least squares*. New York: IEP.

ROMPOS. (n.d.). Coordinate systems: Romanian Position Determination System. National Agency for Cadastre and Land Registration / National Center for Cartography. Retrieved May 18, 2026, from https://rompos.ro/index.php/en/technical-info/coordinate-systems

Sillard, P., & Boucher, C. (2001). A review of algebraic constraints in terrestrial reference frame datum definition. *Journal of Geodesy*, 75(2), 63–73. https://doi.org/10.1007/s001900100166

Takasu, T., & Yasuda, A. (2009). Development of the low-cost RTK-GPS receiver with an open-source program package RTKLIB. *International Symposium on GPS/GNSS.*

Teunissen, P. J. G. (2000). Testing theory: An introduction. Delft University Press.

Triggs, B., McLauchlan, P., Hartley, R., & Fitzgibbon, A. (2000). Bundle adjustment: A modern synthesis. In B. Triggs, A. Zisserman, & R. Szeliski (Eds.), *Vision algorithms: Theory and practice* (pp. 298–372). Springer.

van Mierlo, J. (1980). *Free network adjustment and S-transformations*. Deutsche Geodätische Kommission (DGK), Reihe B, 252.

Verhagen, S. (2005). *GNSS integer ambiguities: Estimation and validation* (Doctoral dissertation). Delft University of Technology.